Solar RRL
www.solar-rrl.com

The Future of Spirobifluorene-Based Molecules as Hole-Transporting Materials for Solar Cells

*Luca Vaghi and Fabio Rizzo**

Organic–inorganic halide perovskite solar cells (PSCs) and organic solar cells (OSCs) attract great attention as alternative renewable photovoltaic technology. The state-of-the-art spiro-OMeTAD (2,2′,7,7′-tetrakis-(*N,N*-di-*p*-methoxyphenylamine)-9,9′-spirobifluorene) is the most successful hole-transport material (HTM) employed in PSCs, whereas solution-processed inverted OSCs generally use poly(3,4-ethylenedioxythiophene):poly(styrenesulfonate) (PEDOT:PSS). Recently, various types of spirobifluorene-based organic small molecules are reported to overcome the known disadvantages of spiro-OMeTAD, such as the complex synthetic route, high synthetic cost, and requirement for hygroscopic dopants to improve the charge-carrier mobility and device performance. Examples of spirobifluorene-based molecules are also reported as alternative HTMs in inverted OSCs to exceed the drawbacks of PEDOT:PSS, such as acidity and batch-to-batch reproducibility. These features significantly limit spiro-OMeTAD and PEDOT:PSS for large-scale application in the future. Herein, an overview of recent developments in spirobifluorene organic small molecules as HTM in PSCs and OSCs is provided by focusing on synthetic and electrical features. Finally, the further research directions are discussed to develop novel spirobifluorene-based HTMs for the realization of reliable and long-term stable photovoltaic devices.

1. Introduction

Renewable energy appears as one of the fundamental points to establish a sustainable society in the next future throughout the production of eco-friendly electricity. Among the renewable resources of energy, solar energy appears as the most abundant, well worldwide distributed and unlimited source of energy. Solar cells, that is, devices, able to convert solar energy into electricity have been developed since long-time. Crystalline Si-based solar cells are the most commercially diffused technologies, showing with the highest power conversion efficiency (PCE) of 26.6%.[1] The cost of the production of Si-based solar cells is significantly reduced in recent years, however, new technologies are necessary to produce solar cells at even lower costs with lower environmental impact. Next-generation technologies, such as dye-sensitized solar cells, quantum dot solar cells, and organic solar cells (OSCs), have emerged in the last decades to replace cost-effective Si-based solar cells. However, their PCEs and long-term stability are still lower than Si-based solar cells, even if the hybrid perovskite solar cells (PSCs) exhibit a continuous improvement in the recent years.[2]

The emerging photovoltaic devices are generally made by multilayers structure, so their efficiency can be improved by acting on every material used on the different layers. In addition to the active layer, which incorporates the material collecting the solar radiation, the charge transport layers are pivotal on the photovoltaic performance. Indeed, hole- and electron-transporting layers (HTL and ETL) transfer the separated charge carriers at the electrodes by avoiding the recombination inside the device. In OSCs, hole-transport materials (HTMs) have usually polymeric nature, such as the poly(3,4-ethylenedioxythiophene):poly(styrenesulfonate) (PEDOT:PSS), but the use of small molecules is increasing due to their chemical versatility and easiest synthesis. Noteworthy, the most used polymeric HTM PEDOT:PSS suffers of instability and induces corrosion on electrodes due to its acidity.

Among the small-molecule HTMs, 2,2′,7,7′-tetrakis-(*N,N*-di-4-methoxyphenylamino)-9,9′-spirobifluorene (spiro-OMeTAD) (**Figure 1**) emerged as the most widely used small molecule in organic photovoltaic devices, first as solid electrolyte in dye-sensitized solar cells[3] and later in PSCs.[4] The pivotal role of spiro-OMeTAD in PSCs is underlined by the impressive certified

L. Vaghi
Department of Materials Science
Università degli Studi di Milano-Bicocca
Via R. Cozzi 55, 20125 Milan, Italy

F. Rizzo
Center for Soft Nanoscience (SoN)
Westfälische Wilhelms-Universität Münster
Busso-Peus-Str. 10, 48149 Münster, Germany

F. Rizzo
Institute of Chemical Science and Technologies "G. Natta" (SCITEC)
National Research Council (CNR)
via G. Fantoli 16/15, 20138 Milan, Italy
E-mail: fabio.rizzo@cnr.it

The ORCID identification number(s) for the author(s) of this article can be found under https://doi.org/10.1002/solr.202201108.

© 2023 The Authors. Solar RRL published by Wiley-VCH GmbH. This is an open access article under the terms of the Creative Commons Attribution-NonCommercial License, which permits use, distribution and reproduction in any medium, provided the original work is properly cited and is not used for commercial purposes.

DOI: 10.1002/solr.202201108

Check for updates
2367198x, 0, Downloaded from https://onlinelibrary.wiley.com/doi/10.1002/solr.202201108 by University Studi Milano Bicocca, Wiley Online Library on [22/02/2023]. See the Terms and Conditions (https://onlinelibrary.wiley.com/terms-and-conditions) on Wiley Online Library for rules of use; OA articles are governed by the applicable Creative Commons License

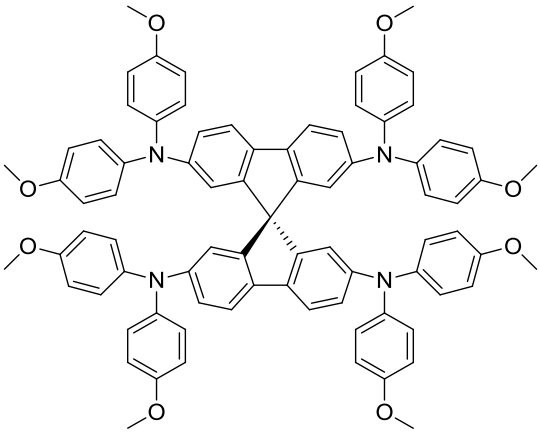

Figure 1. Molecular structure of 2,2′,7,7′-tetrakis-(*N*,*N*-di-4-methoxyphenylamino)-9,9′-spirobifluorene (spiro-OMeTAD).

PCE values above 25% recorded in the past years by using this HTM in the photovoltaic devices.[5] However, spiro-OMeTAD suffers from low stability, high production cost, and low hole mobility, thus many efforts have been devoted to find valuable alternative small molecules as HTMs.[6] Although many organic HTMs have been reported in the past years,[7] there is still a need to evaluate and assess improvement of the performance of organic HTLs in solar cells. Particular attention has been devoted to develop HTMs integrating a spiro-unit to benefit of high melting point, which provides powerful support for the thermal stability of the devices.

Herein, we discuss the most recent progress on the research of spirobifluorene derivatives as alternative HTMs in next-generation solar cells, by emphasizing the synthetic and stability features. The aim is to stimulate researchers to develop spirobifluorene-based HTMs with improved performance for both PSCs and OSCs.

2. Beyond Spiro-OMeTAD's Limitations

The spiro-type HTMs are widely used due to the merits of the spiro-linked architectures, such as nonplanar 3D geometry, high-glass-transition temperature (T_g), and good solubility due to weak intermolecular π–π interactions.[8] In the spirobifluorene, the two fluorene halves connected by a sp^3-hybridized carbon form a cross-shape molecular configuration, which induces high rigidity and reduces the aggregation during the film-formation process. These features stimulated researchers to overcome the high performance obtained by spiro-OMeTAD by investigating other spirobifluorene-based HTMs in organic (bulk heterojunction, BHJ) and hybrid organic/inorganic (perovskite, PSC) solar cells. An adopted strategy to overcome the low hole mobility of the spiro-OMeTAD is the addition of dopant species, such as LiTFSI—bis(trifluoromethane)sulfonimide lithium salt and 4-tert-butyl pyridine (tBP).[9] However, the strong tendency to crystallization and enhanced π–π stacking could help HTMs to extract carriers efficiently, and dopants are prone to aggregate around the grain boundary, leading to the precipitation of Li salts or the formation of pinholes in the film.[9,10] Moreover, the possible interaction of tBP with the oxidized form of spiro-OMeTAD is also causing decrease on the efficiency of the photovoltaic devices.[11] Although the introduction of other additives such as PbS nanocrystals[12] and alkylthiol[13] allows enhancing the long-term stability of the PSCs, this perspective will focus on the development of novel molecular HTMs based on the spirobifluorene core.

2.1. Recent Advances (2021–2022)

To overcome the limits of the benchmark (spiro-OMeTAD) in PSCs, different molecular design on the spirobifluorene core have been investigated. The properties of the discussed HTMs are summarized in **Table 1**.

The approach involving the partial substitution of the phenyl ring on the amine was first presented in 2018 by Seo, Lee, and coworkers, which reached an enhancement of the PCE value as well as of the thermal stability by replacing one methoxyphenyl unit per amine with a fluorene (**DM**).[14] This strategy has been successfully used by other research groups using different extended aromatic systems instead of fluorene (**Figure 2**). In 2021, Chen et al. reported two analogous of spiro-OMeTAD with the partial substitution of the methoxyphenyl terminal groups with either *N*-ethyl-carbazole (**SC**) or dibenzothiophene (**ST**).[15] Both **SC** and **ST** show energy highest occupied molecular orbital (HOMO) level lower than the benchmark (−5.26 and −5.31 eV vs −5.22 eV by cyclic voltammetry, −5.09 and −5.17 eV vs −5.05 eV in solid state), which improves the hole injection from the perovskite layer. Interestingly, the behavior of both compounds was different during the film deposition, which influenced the parameters of the photovoltaic devices. Indeed, **ST** showed high crystallinity and poor solubility, resulting in the formation of pinholes in the film due to the undissolved molecules and the aggregation of the dopant Li-TFSI. On the contrary, **SC** had low crystallinity and high solubility, leading to the formation of homogeneous film with good distribution of the dopant. For comparison, spiro-OMeTAD shows high solubility but high crystallinity, which induces aggregation of Li salts and their precipitation during the film formation. By following the same strategy, Liang et al. used dibenzofuran or dibenzothiophene as the terminal group to prepare two new HTMs for PSCs, that is, **spiro-DBF** and **spiro-DBT**.[16] Both compounds show HOMO level (−5.22 eV) lower than the benchmark, and low PCE for dopant-free devices (7.68% and 10.09% for **spiro-DBF** and **spiro-DBT**, respectively). As well for spiro-OMeTAD, the presence of dopants enhances the performance of the solar cells, which reached PCE around 19–20% similar to the reference device. The hole mobilities of **spiro-DBF** ($6.31 \times 10^{-3}\,cm^2\,V^{-1}\,s^{-1}$) and **spiro-BDT** ($1.25 \times 10^{-3}\,cm^2\,V^{-1}\,s^{-1}$) are on the same order of that of the spiro-OMeTAD ($2.87 \times 10^{-3}\,cm^2\,V^{-1}\,s^{-1}$), even if for the spiro-OMeTAD the authors obtained a hole mobility value ten time higher than that reported in literature for the same compound.[17] The long-term stability of the photovoltaic devices with the novel HTMs is higher than the solar cell with the standard HTM, as demonstrated by the experiments carried out at high humidity conditions (60% relative humidity). Unfortunately, the authors did not report annealing experiments performed at high temperatures.

© 2023 The Authors. Solar RRL published by Wiley-VCH GmbH

2367198x, 0, Downloaded from https://onlinelibrary.wiley.com/doi/10.1002/solr.202201108 by University Studi Milano Bicocca, Wiley Online Library on [22/02/2023]. See the Terms and Conditions (https://onlinelibrary.wiley.com/terms-and-conditions) on Wiley Online Library for rules of use; OA articles are governed by the applicable Creative Commons License

Table 1. A summary of the properties of the spirobifluorene-based HTMs.

HTM	HOMO [eV]	μ_h [$cm^2 V^{-1} s^{-1}$]	Solar cell	PCE [%]	Ref.
Spiro-OMeTAD	−4.81	2×10^{-4} a)	FTO/c-TiO_2/mp-TiO_2/$MAPbI_3$/HTM/Au	12.9	[27]
Spiro-OMeTAD doped	−5.10	6.503×10^{-3}	FTO/c-TiO_2/mp-TiO_2/$FAPbI_3$/HTM/Au	24.89	[18]
SC	−5.26	3.15×10^{-3}	FTO/SnO_2/$(CsPbI_3)_x(FAPbI_3)_y(MAPbBr_3)_{1-x-y}$/HTM/Ag	21.76	[15]
ST	−5.31	1.77×10^{-3}	FTO/SnO_2/$(CsPbI_3)_x(FAPbI_3)_y(MAPbBr_3)_{1-x-y}$/HTM/Ag	18.18	[15]
Spiro-DBF	−5.22	6.31×10^{-3}	FTO/bl-TiO_2/mp-TiO_2/$(CsPbI_3)_{0.05}(FAPbI_3)_{0.95}$/HTM/Au	21.43	[16]
Spiro-DBT	−5.22	1.25×10^{-3}	FTO/bl-TiO_2/mp-TiO_2/$(CsPbI_3)_{0.05}(FAPbI_3)_{0.95}$/HTM/Au	20.37	[16]
Spiro-Naph	−5.15	8.084×10^{-3}	FTO/c-TiO_2/mp-TiO_2/$FAPbI_3$/HTM/Au	25.40	[18]
Spiro-mF-Naph	−5.34	–	FTO/c-TiO_2/mp-TiO_2/$FAPbI_3$/HTM/Au	23.68	[18]
Spiro-ON	−5.33	–	FTO/c-TiO_2/mp-TiO_2/$FAPbI_3$/HTM/Au	19.80	[18]
Spiro-OP	−5.31	–	FTO/c-TiO_2/mp-TiO_2/$FAPbI_3$/HTM/Au	20.36	[18]
Spiro-4TFETAD	−5.33	2.04×10^{-4}	ITO/SnO_2/$(FAPbI_3)_{0.97}(MAPbBr_3)_{0.03}$/HTM/Ag	21.11	[20]
Spiro-OHTAD	−5.02	–	ITO/SnO_2/$(FAPbI_3)_{0.97}(MAPbBr_3)_{0.03}$/HTM/Au	20.11	[21]
Spiro-SMeTAD	−5.25	1.90×10^{-5} b)	FTO/bl-TiO_2/mp-TiO_2/$Cs_{0.05}(FA_{0.85}MA_{0.15})_{0.95}Pb(I_{0.85}Br_{0.15})_3$/HTM/Au	16.39	[22]
Spiro-OSMeTAD	−5.18	–	FTO/bl-TiO_2/mp-TiO_2/$Cs_{0.05}(FA_{0.85}MA_{0.15})_{0.95}Pb(I_{0.85}Br_{0.15})_3$/HTM/Au	18.24	[22]
V1305	−5.33	1.7×10^{-5}	FTO/c-TiO_2/*m*-TiO_2/SnO_2/$[(FAPbI_3)_{0.87}(MAPbBr_3)_{0.13}]_{0.92}(CsPbI_3)_{0.08}$/HTM/Au	19.0	[24]
V1306	−5.37	5.4×10^{-6}	FTO/c-TiO_2/*m*-TiO_2/SnO_2/$[(FAPbI_3)_{0.87}(MAPbBr_3)_{0.13}]_{0.92}(CsPbI_3)_{0.08}$/HTM/Au	15.8	[24]
V1307	−5.46	6.4×10^{-4}	FTO/c-TiO_2/*m*-TiO_2/SnO_2/$[(FAPbI_3)_{0.87}(MAPbBr_3)_{0.13}]_{0.92}(CsPbI_3)_{0.08}$/HTM/Au	19.2	[24]
V1308	−5.46	9.4×10^{-4}	FTO/c-TiO_2/*m*-TiO_2/SnO_2/$[(FAPbI_3)_{0.87}(MAPbBr_3)_{0.13}]_{0.92}(CsPbI_3)_{0.08}$/HTM/Au	19.1	[24]
V1267	5.07c)	3.6×10^{-4} d)	FTO/c-TiO_2/*m*-TiO_2/SnO_2/$[(FAPbI_3)_{0.87}(MAPbBr_3)_{0.13}]_{0.92}(CsPbI_3)_{0.08}$/HTM/Au	18.3	[25]
V1240	5.15c)	5.6×10^{-6} d)	FTO/c-TiO_2/*m*-TiO_2/SnO_2/$[(FAPbI_3)_{0.87}(MAPbBr_3)_{0.13}]_{0.92}(CsPbI_3)_{0.08}$/HTM/Au	17.6	[25]
V1222	5.16c)	3.9×10^{-4} d)	FTO/c-TiO_2/*m*-TiO_2/SnO_2/$[(FAPbI_3)_{0.87}(MAPbBr_3)_{0.13}]_{0.92}(CsPbI_3)_{0.08}$/HTM/Au	15.7	[25]
V1226	5.16c)	3.8×10^{-5} d)	FTO/c-TiO_2/*m*-TiO_2/SnO_2/$[(FAPbI_3)_{0.87}(MAPbBr_3)_{0.13}]_{0.92}(CsPbI_3)_{0.08}$/HTM/Au	15.7	[25]
V1238	5.16c)	1.8×10^{-5} d)	FTO/c-TiO_2/*m*-TiO_2/SnO_2/$[(FAPbI_3)_{0.87}(MAPbBr_3)_{0.13}]_{0.92}(CsPbI_3)_{0.08}$/HTM/Au	16.1	[25]
V1257	5.08c)	3.6×10^{-5} d)	FTO/c-TiO_2/*m*-TiO_2/SnO_2/$[(FAPbI_3)_{0.87}(MAPbBr_3)_{0.13}]_{0.92}(CsPbI_3)_{0.08}$/HTM/Au	17.2	[25]
V1258	5.08c)	1.2×10^{-5} d)	FTO/c-TiO_2/*m*-TiO_2/SnO_2/$[(FAPbI_3)_{0.87}(MAPbBr_3)_{0.13}]_{0.92}(CsPbI_3)_{0.08}$/HTM/Au	17.8	[25]
V1269	5.08c)	3×10^{-5} d)	FTO/c-TiO_2/*m*-TiO_2/SnO_2/$[(FAPbI_3)_{0.87}(MAPbBr_3)_{0.13}]_{0.92}(CsPbI_3)_{0.08}$/HTM/Au	18.1	[25]
Spiro-carbazole	−5.15	6.48×10^{-3}	FTO/bl-TiO_2/mp-TiO_2/$Cs_{0.05}FA_{0.95}PbI_3$/HTM/Au	22.01	[26]
SF-27	−4.90	0.5×10^{-5}	FTO/c-TiO_2/mp-TiO_2/$MAPbI_3$/HTM/Au	7.6	[27]
SF48	−4.83	1.7×10^{-5}	FTO/c-TiO_2/mp-TiO_2/$MAPbI_3$/HTM/Au	16.3	[27]
			FTO/c-TiO_2/mp-TiO_2/$Cs_{0.05}(FA_{0.85}MA_{0.15})_{0.95}Pb(I_{0.89}Br_{0.11})_3$/HTM/Au	18.7	
Spiro-PT	−5.66	1.68×10^{-4}	FTO/TiO_2/$MAPbBr_{3-x}Cl_x$/HTM/Au	7.90	[28]
CF-Sp-Th	−5.38	3.14×10^{-5}	FTO/HTM/GO(0.5 wt%)-$MAPbI_3$/$PC_{61}BM$/Au	14.28	[30]
Isomer 1	−5.32	4.1×10^{-3}	ITO/ZnO/PTB7-Th:ITIC/HTM/Ag	5.48	[31]
			ITO/ZnO/PBDB-T-2Cl:Y6/HTM/Ag	8.33	
Isomer 2	−5.33	3.5×10^{-3}	ITO/ZnO/PTB7-Th:ITIC/HTM/Ag	5.65	[31]
			ITO/ZnO/PBDB-T-2Cl:Y6/HTM/Ag	7.79	

a)From Ref. [17]; b)from Ref. [23]; c)oxidation potential in solution; d)hole drift mobility values extrapolated by measurements of HTM mixed with Z-polycarbonate polymer binder.

In 2022, Yang et al. showed that the use of naphthyl substituents enhances the performance and stability of doped PSCs with conventional architecture (**Figure 3**).[18] The authors reported four new compounds (**spiro-Naph**, **spiro-ON**, **spiro-OP**, and **spiro-*m*F-Naph**) with different substituents on the phenyl or naphthyl units of the amines. By comparing the dyes, the presence of methoxy groups on both phenyl and naphthyl substituents allows recording open-circuit voltage (V_{oc}) exceeding 1.10 V and short-circuit current density (J_{sc}) higher than 25 mA cm^{-2}. Furthermore, the presence of a fluorine atom in meta-position on the methoxyphenyl ring in **spiro-mF-Naph** keeps the fill factor (FF) value below 80% compared to the most efficient **spiro-Naph**. Interestingly, **spiro-ON**, **spiro-OP**, and **spiro-*m*F-Naph** have HOMO levels too deep (between −5.31 and −5.34 eV) to transport efficiently the hole carriers from the $FAPbI_3$ perovskite. The photovoltaic device made with **spiro-Naph** shows a PCE value of 23.59% (a certified 21.83% for a 25 cm^2 large-area PSC), which is larger than the control spiro-OMeTAD-based device. Noteworthy,

© 2023 The Authors. Solar RRL published by Wiley-VCH GmbH

2367198x, 0, Downloaded from https://onlinelibrary.wiley.com/doi/10.1002/solr.202201108 by University Studi Milano Bicocca, Wiley Online Library on [22/02/2023]. See the Terms and Conditions (https://onlinelibrary.wiley.com/terms-and-conditions) on Wiley Online Library for rules of use; OA articles are governed by the applicable Creative Commons License

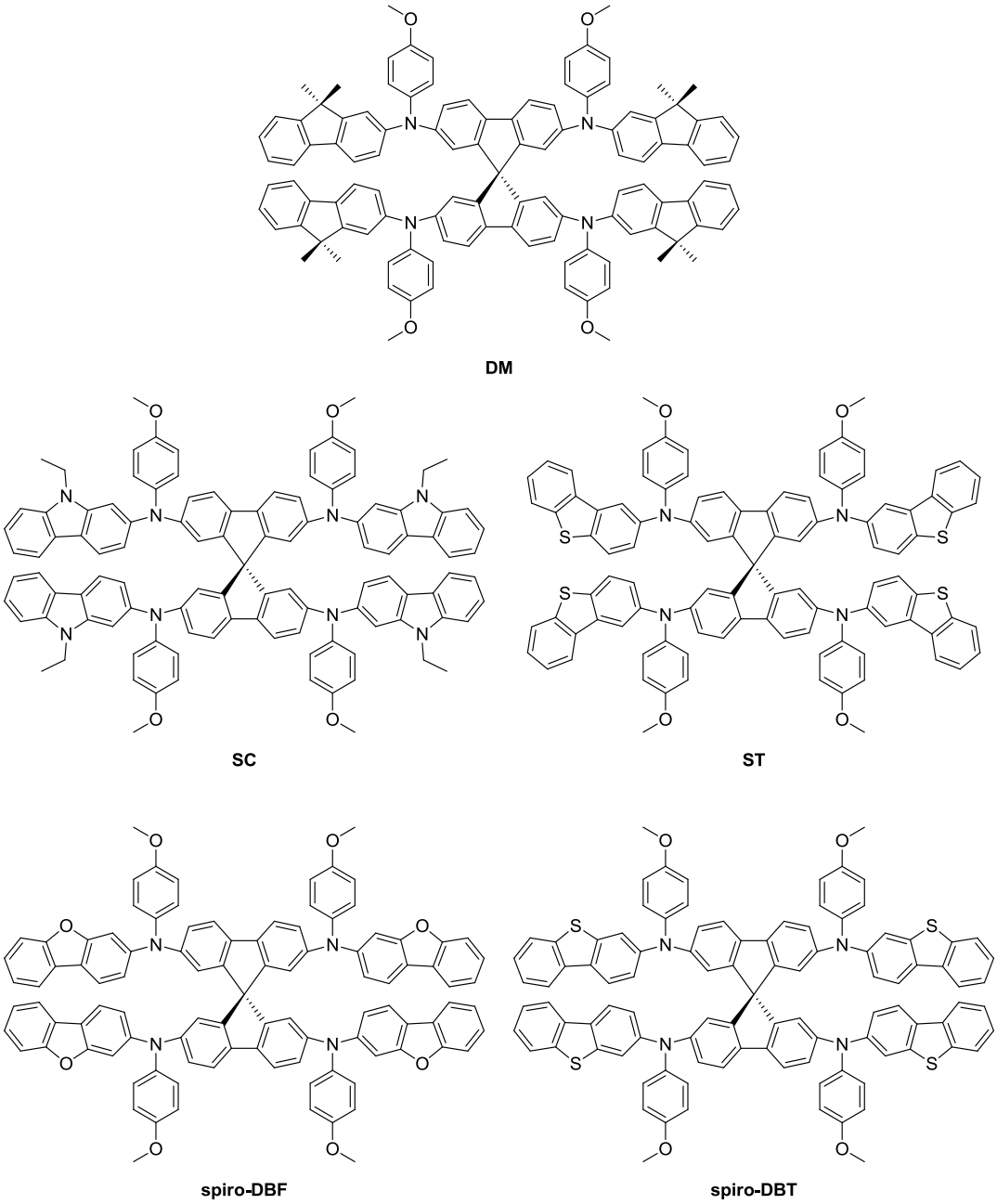

Figure 2. Structure of **DM**, **SC**, **ST**, **spiro-DBF**, and **spiro-DBT**.

the long-term stability with 60 °C thermal condition of the **spiro-Naph** device (PCE 18.79% after 400 h) was higher than the corresponding photovoltaic devices made with spiro-OMeTAD (11.78%) and with **spiro-mF** (14.74%), another spirobifluorene-based HTM published in 2020 by the same authors.[19]

Another strategy to improve the performance of PSCs with conventional architecture is based on the enhancement of the hydrophobicity of the HTM. Guo, Yan, and coworkers reported the study on the fluorinated isomeric analog of the spiro-OMeTAD called **spiro-4TFETAD**, bearing a partial substitution of methoxy substituents with trifluoroethoxy groups (**Figure 4**).[20] The effect of the substitution in the increase of the T_g value (140 °C) and hole mobility ($2.04 \times 10^{-4}\,cm^2\,V^{-1}\,s^{-1}$), together with a lower HOMO level (−5.25 eV). The improved hydrophobicity of **spiro-4TFETAD** allows higher protection of the perovskite layer toward moisture for PSCs with conventional architecture, resulting in an overall improvement of the long-term stability of the solar cells. Indeed, under 60% relative humidity the **spiro-4TFETAD**-based PSCs maintained 83% of the initial performance after 250 h aging test without encapsulation, whereas the authors recorded a decrease to 70% for the benchmark PSCs. The best PCE exceeding 21% was obtained by doping the HTL, which lowers the

© 2023 The Authors. Solar RRL published by Wiley-VCH GmbH

2367198x, 0, Downloaded from https://onlinelibrary.wiley.com/doi/10.1002/solr.202201108 by University Studi Milano Bicocca, Wiley Online Library on [22/02/2023]. See the Terms and Conditions (https://onlinelibrary.wiley.com/terms-and-conditions) on Wiley Online Library for rules of use; OA articles are governed by the applicable Creative Commons License

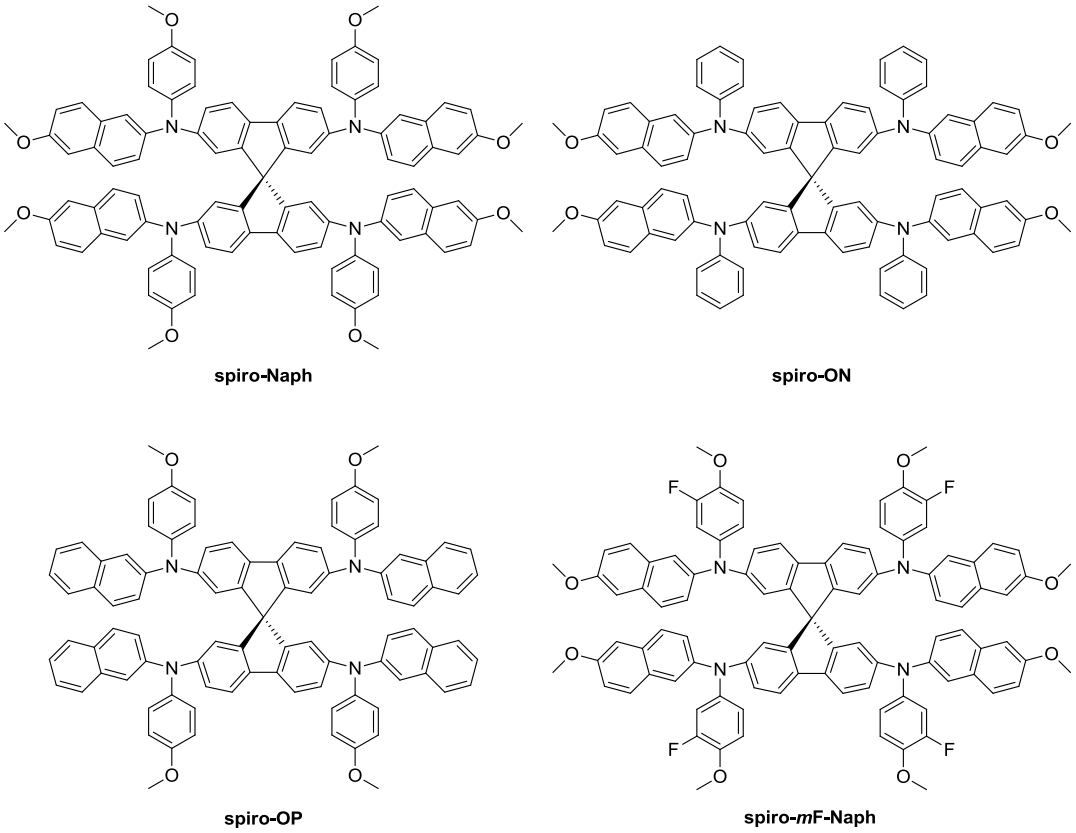

Figure 3. Structure of **spiro-Naph**, **spiro-ON**, **spiro-OP**, and **spiro-*m*F-Naph**.

HOMO level of the spiro-compound compared to the dopant-free material.

In addition, the approach involving the modification of all lateral phenyl rings of spiro-OMeTAD is another valuable strategy to improve the stability of solar cells (Figure 4). By changing the methoxy groups with hydroxyl substituents, Li et al. recently reported PCE > 20% in PSCs with improved thermal stability under ambient conditions.[21] These results arise from the hydrogen bonding that OH groups form with the perovskite. The outcome is the stabilization of the defects on the perovskite surface, such as uncoordinated lead ions, mobile formamidine cations, and halogen anions, which leads to an enhancement of the stability of the device. However, the passivation species **spiro-OHTAD** is obtained by demethylation of the spiro-OMeTAD, thus the authors did not overcome the problem of the cost of the HTMs. Furthermore, the proposed synthetic procedure involved the use of boron tribromide, a highly toxic and corrosive compound with dangerous environmental impact that hampers its large-scale use. Other two HTMs for doped PSCs reported by Zhang et al. involved the partial or complete replacement of oxygen atoms of spiro-OMeTAD with sulfur (**spiro-OSMeTAD** and **spiro-SMeTAD**, respectively).[22] The use of a different chalcogenide than oxygen increases the T_g values, thus improves the thermal stability of the molecules. However, **spiro-SMeTAD** exhibits bad tolerance for dopants during the film formation, which affects the performance of the device with a PCE of 16.39%. Interestingly, the compound with four methylsulfanyl groups was previously employed in inverted PSCs displaying a PCE of 15.92% and hole mobility of 1.90×10^{-5} cm^2 V^{-1} s^{-1}.[23] On the contrary, the presence of both chalcogenide atoms in **spiro-OSMeTAD** has positive effect on the device with 18.24% PCE (18.18% by using commercial spiro-OMeTAD), arising from a slightly lower HOMO level than spiro-OMeTAD (−5.18 eV vs −5.10 eV) that enhances the charge transport.

In 2021, Nazeeruddin, Getautis, and coworkers reported a series of four spirobifluorene derivatives (**V1305**, **V1306**, **V1307**, and **V1308**) bearing one to four enamine groups introduced by simple condensation reaction (**Figure 5**).[24] Very interestingly, the performance of di- or tetra-substituted spiro-compounds was comparable in terms of PCE and stability, indicating that the double substitution of spirobifluorene can be a valuable strategy to reduce the complexity of the synthesis and then the cost of production. The adopted synthetic strategy avoids the use of metal catalysts during the last reaction step, thus reducing the general costs to synthetize the HTMs. However, the starting intermediates employed in place of the bromo-derivatives are the amino-spirobifluorenes, which determine the high costs of the new compounds (even if lower than the spiro-OMeTAD). The investigated PSCs reach a maximum PCE of 19.2% and a stability comparable to spiro-OMeTAD by fabricating the devices with conventional architecture and in presence of dopants. However, the hole mobility of the four compounds range between 5.4×10^{-6} and 9.4×10^{-4} cm^2 V^{-1} s^{-1}, indicating that further improvement must be done to enhance the hole-transporting character of the enamine-based HTMs.

© 2023 The Authors. Solar RRL published by Wiley-VCH GmbH

2367198x, 0, Downloaded from https://onlinelibrary.wiley.com/doi/10.1002/solr.202201108 by University Studi Milano Bicocca, Wiley Online Library on [22/02/2023]. See the Terms and Conditions (https://onlinelibrary.wiley.com/terms-and-conditions) on Wiley Online Library for rules of use; OA articles are governed by the applicable Creative Commons License

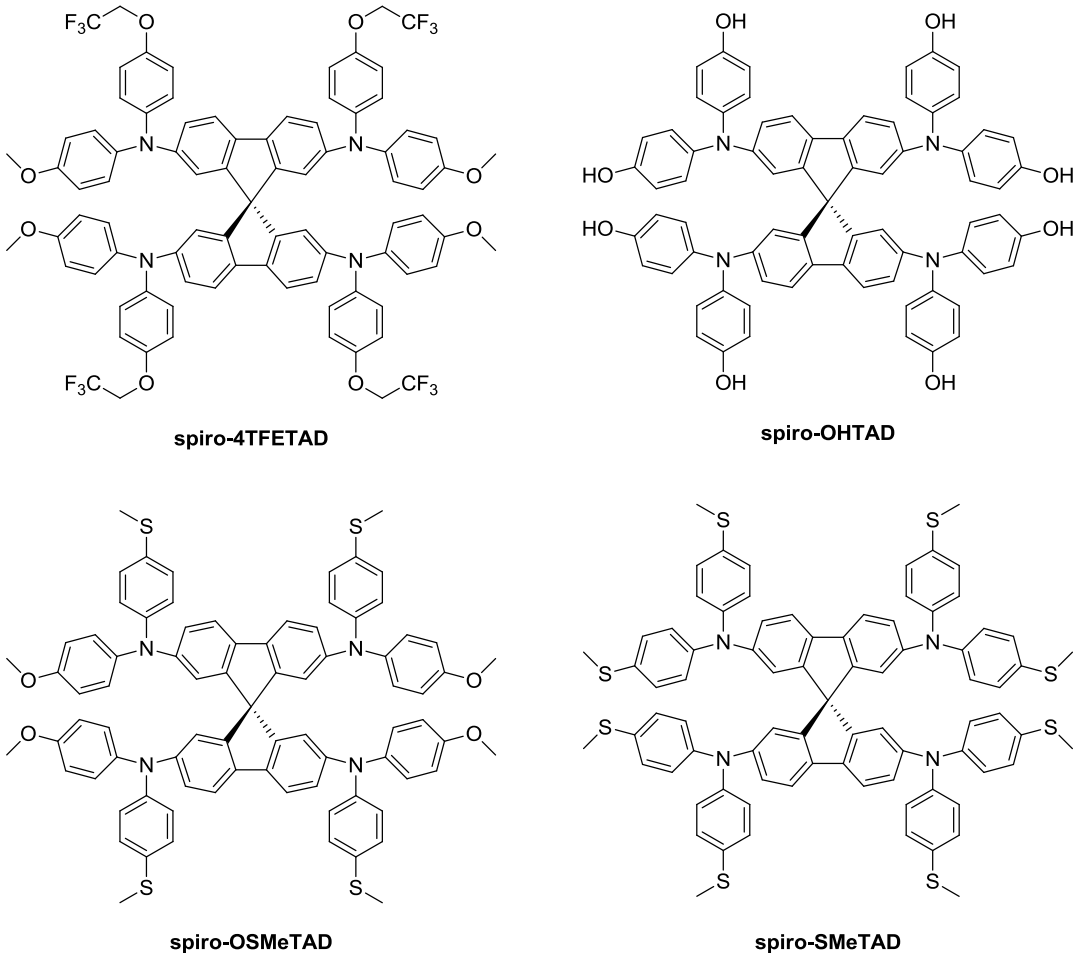

Figure 4. Structure of **spiro-4TFETAD**, **spiro-OHTAD**, **spiro-OSMeTAD**, and **spiro–SMeTAD**.

The same authors reported the tetra-substituted spirobifluorene either with *N*-ethylcarbazole terminal groups instead of the methoxyphenyl moieties (**V1267**) or with the partial replacement (**V1240**).[25] The two novel compounds exhibit similar performance for doped PSCs, with PCE around 18%. In addition, the authors carried out the comparison with fluorene-based molecules bearing the same lateral substituents as "half" molecules, which benefit of an easier synthesis. Very interestingly, the performance of PSCs with the fluorene derivatives (**V1222**, **V1226**, **V1238**, **V1257**, **V1258**, **V1269**) is comparable with the spirobifluorene-based compounds in terms of PCE (between 15.7% and 18.1%) and long-term stability.

The substitution of the four methoxyphenyl terminal groups with *N*-ethylcarbazole has been reported also from another research group, but attached in another position compared to **V1267**.[26] Indeed, the **spiro-carbazole** displays the *N*-ethylcarbazole attached in position 2 to the core, whereas in **V1267** the same substituent is linked in position 3 to the spirobifluorene. The HTM exhibits an improvement of the PCE of PSCs with n–i–p (conventional) architecture up to 22.01% compared to the reference spiro-OMeTAD (21.12%), thus slightly better than the aforementioned regioisomer. The **spiro-carbazole** presents higher T_g, better device humidity, and thermal stability compared to the control device. However, the investigated compound needs to be used in doped layer to show high PCE, which enhances the complexity of the production processes of solar cells in large scale. Compared to the preparation of the regioisomer **V1267**, the synthesis of **spiro-carbazole** involves the more expensive 9,9′-spirobifluorene-2,2′,7,7′-tetraamine as starting material.

Solar cells employing dopant-free HTMs are attracting because of easier production processes and reduction of the costs. Among the most recent examples, Murakami and coworkers reported a tetrasubstituted spirobifluorene derivative as efficient dopant-free HTM for PSCs with conventional architecture.[27] In comparison with the compound **Spiro-N** bearing *N*, *N*-dimethylamino groups to replace the methoxy groups,[27] the authors introduced two cyano groups into the dimethylamino-substituted rings in meta- or ortho-positions (**SF27** and **SF48**, respectively) of the nitrogen atom attached to the spirobifluorene core (**Figure 6**). The presence of strong electron-withdrawing groups lowers the HOMO energies and induces dipoles, which facilitate charge transfer and intermolecular interactions, together with a passivation effect due to the coordination of

© 2023 The Authors. Solar RRL published by Wiley-VCH GmbH

2367198x, 0, Downloaded from https://onlinelibrary.wiley.com/doi/10.1002/solr.202201108 by University Studi Milano Bicocca, Wiley Online Library on [22/02/2023]. See the Terms and Conditions (https://onlinelibrary.wiley.com/terms-and-conditions) on Wiley Online Library for rules of use; OA articles are governed by the applicable Creative Commons License

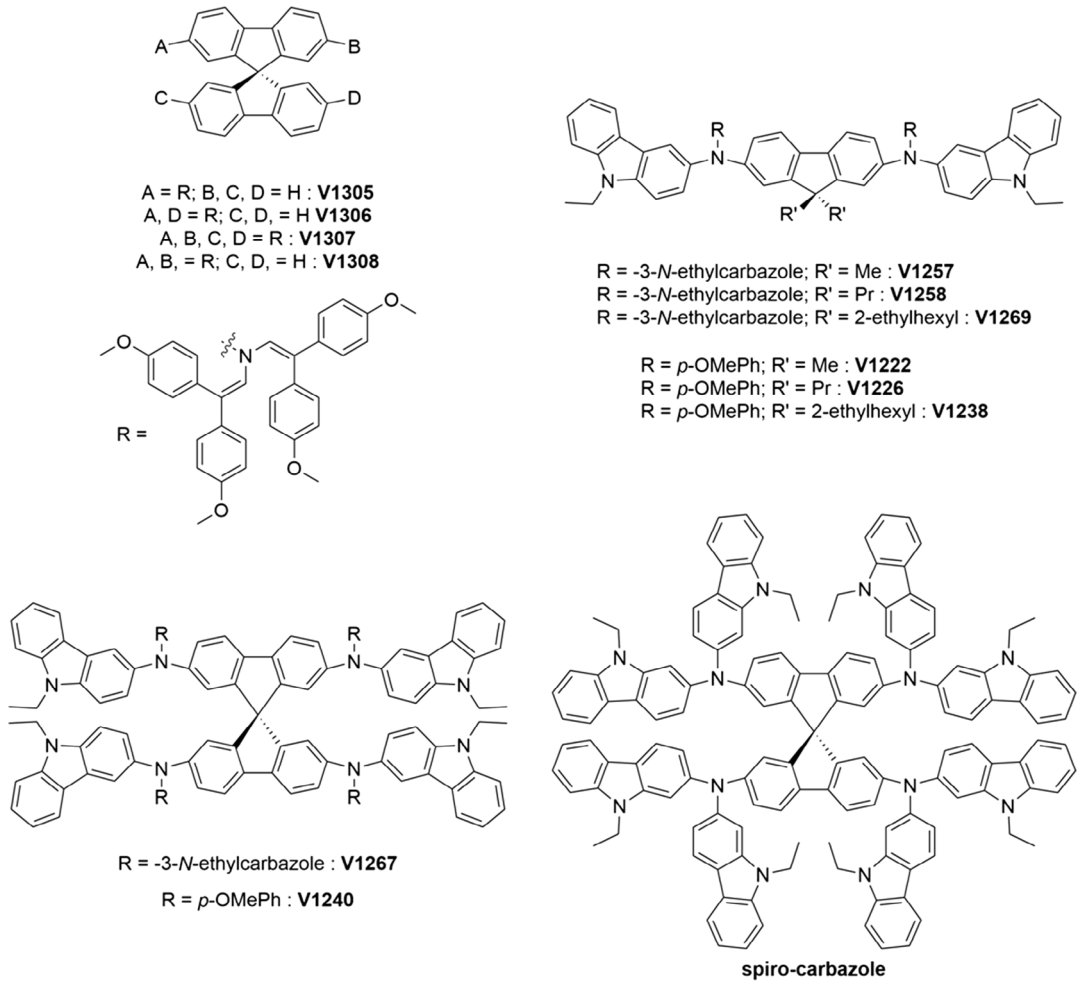

Figure 5. Structure of **V1305**, **V1306**, **V1307**, **V1308**, **V1257**, **V1258**, **V1269**, **V1222**, **V1226**, **V1238**, **V1267**, **V1240**, and **spiro-carbazole**.

the cyano group to lead ions. Both compounds exhibit good thermal stability verified by checking the NMR spectra before and after heating the sample at 280 °C, and hole mobility values (0.5 and 1.7×10^{-5} $cm^2 V^{-1} s^{-1}$ for **SF27** and **SF48**, respectively) ten times lower than the spiro-OMeTAD. The authors overcame this disadvantage by depositing thin HTL (≈50 nm) on the perovskite film. Under these conditions, the best PCE obtained for dopant-free devices is 16.3% for **SF48**, while the dopant-free spiro-OMeTAD shows only 12.9%. Very interestingly, the dopant-free PSCs with **SF48** exhibits good stability by keeping over 90% of the maximum PCE after storage for 800 h in air at 85 °C, which is much higher than the outcomes obtained with doped- and dopant-free spiro-OMeTAD solar cells. Moreover, the authors showed a further enhancement of PCE up to 18.7% by employing the triple-cation-mixed perovskite. Qin and coworkers reported on the tetra-substituted spirobifluorene with *N*-phenothiazine (**spiro-PT**).[28] The compound show a low-energy HOMO (−5.66 eV) and a hole mobility (1.68×10^{-4} $cm^2 V^{-1} s^{-1}$) higher than spiro-OMeTAD. The authors employed the new HTM for dopant-free perovskite-based wide-bandgap photovoltaics (WBPV) with conventional architecture, which can be applied to fabricate smart windows on facades. The measured PCE for the WBPV device is 7.90% that improves the 6.79% displayed by using the benchmark. Since the WBPV has the advantage to exhibit high V_{oc}, it is worth to emphasize that the **spiro-PT** shows a V_{oc} of 1.41 V (1.36 V for spiro-OMeTAD). Moreover, the stability of the photovoltaic device is greatly enhanced, showing a maximum PCE retention rate of 91% after being stored for nearly 500 h under environmental conditions without encapsulation. In contrast, the device with doped-spiro-OMeTAD has a retention rate of 45% after the same period.

Solar cells with inverted architecture generally exhibit lower PCE value than that with conventional architecture, but recent works showed that it is possible to exceed 21% PCE with dopant-free small-molecule HTM with inverted configuration.[29] However, the literature about HTM spirobifluorene derivatives employed with p–i–n architecture is still poor, indicating the great opportunity to develop this area of research. In 2019, Ameen et al. reported a bi-functionalized spirobifluorene core with a donor–acceptor structure (**CF-Sp-BTh**, Figure 6) as HTM in graphene oxide (GO)-perovskite inverted planar heterojunction solar cells.[30] The dye shows HOMO level at −5.38 eV that is suited for the HOMO of the perovskite (−5.43 eV),

© 2023 The Authors. Solar RRL published by Wiley-VCH GmbH

2367198x, 0, Downloaded from https://onlinelibrary.wiley.com/doi/10.1002/solr.202201108 by University Studi Milano Bicocca, Wiley Online Library on [22/02/2023]. See the Terms and Conditions (https://onlinelibrary.wiley.com/terms-and-conditions) on Wiley Online Library for rules of use; OA articles are governed by the applicable Creative Commons License

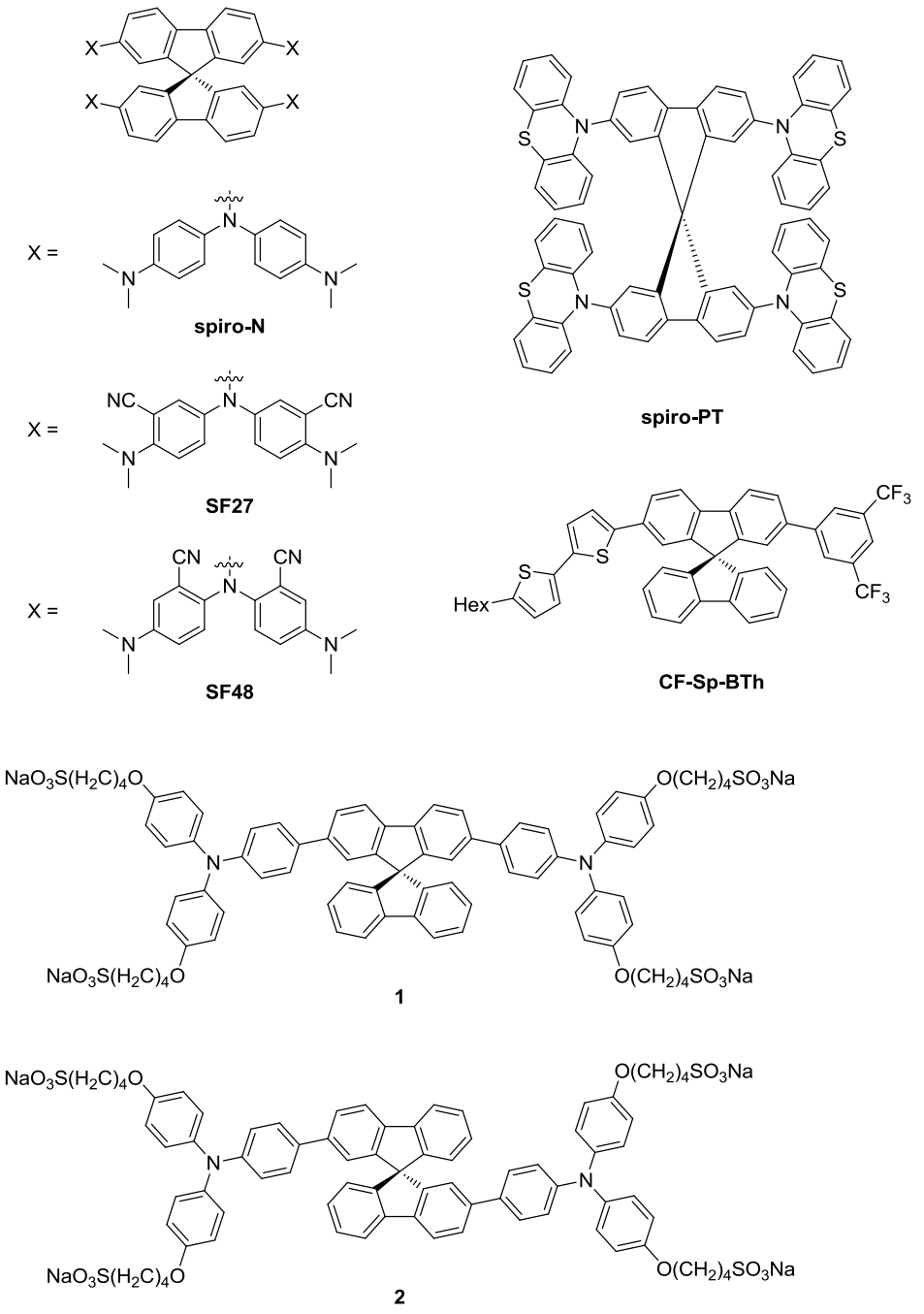

Figure 6. Structure of **spiro-N, SF27, SF48**, **spirobifluorene** with ***N*-phenothiazine** (**spiro-PT**), **CF-Sp-BTh, 1**, and **2**.

resulting in a good charge transport. The photovoltaic device reaches interesting PCE values in presence of GO (14.28%), while the reference device with pristine perovskite has lower performance (PCE 9.2%), indicating the importance of the additive and its concentration. Indeed, the authors showed that the optimal composition for the best performance was 0.5 wt%, whereas lower or higher concentrations of GO had detrimental effects. The GO plays an important role also on the enhancement of the hole mobility compared to the pristine perovskite, which balances the modest hole mobility of **CF-Sp-BTh** ($3.14 \times 10^{-5}\,cm^2\,V^{-1}\,s^{-1}$). It is worth to emphasize that the employment of disubstituted spirobifluorene reduces the synthetic complexity as well as the purification process. Unfortunately, the authors did not perform studies about the stability of the solar cells.

More recently, Rizzo, Vohra, and coworkers reported two regioisomers of spirobifluorene functionalized with triphenylamine groups in 2,7 (compound **1**) or in 2,2′

© 2023 The Authors. Solar RRL published by Wiley-VCH GmbH

2367198x, 0, Downloaded from https://onlinelibrary.wiley.com/doi/10.1002/solr.202201108 by University Studi Milano Bicocca, Wiley Online Library on [22/02/2023]. See the Terms and Conditions (https://onlinelibrary.wiley.com/terms-and-conditions) on Wiley Online Library for rules of use; OA articles are governed by the applicable Creative Commons License

(compound **2**) positions bearing lateral chains terminating with sulfonates that induce solubility in water and alcoholic solvents (Figure 6).[31] The two compounds show very high hole mobility (4.1 and 3.5×10^{-3} $cm^2 V^{-1} s^{-1}$ for **1** and **2**, respectively) due to the presence of the triphenylamine substituents. Noteworthy, these values are one order of magnitude higher than spiro-OMeTAD and PEDOT-PSS, indicating the outstanding ability to act as HTMs, which is also facilitated by the HOMO levels at −5.32 and −5.33 eV measured by photoelectron yield spectroscopy (PYS). The two isomers were investigated as substituted HTM of PEDOT:PSS in BHJ solar cells with inverted architecture in combination with two different active layers, such as PTB7-Th:ITIC and PBDB-T-2Cl:Y6, showing an enhancement up to 28% of the performance of the solar cells compared to the same devices employing PEDOT:PSS. The authors emphasized the stability of the two compounds during the annealing performed at 100 °C and also the very limited oxidative effect observed on the surface of the silver anode. This important drawback is usually observed in inverted BHJ solar cells and arises from the acidity of the PEDOT:PSS. Very important, both isomers **1** and **2** were deposited by spin-coating from an aqueous solution (water/ethanol) that drastically reduced the environmental impact of the production of the devices employing these molecules. The PCE of 8% is reached by employing an easy multilayer structure (Ag anode/HTM/active layer/ZnO/ITO), thus could be further increased by complexity of the device, but it represents actually the highest PCE reported for PEDOT:PSS-free small-molecule inverted solar cells deposited from an aqueous solution.

2.2. Synthesis

In addition to the final device performances, the sustainability and cost-effectiveness of synthetic pathways to spirobifluorene-based HTMs play a key role toward the jump from basic research to large-scale industrial production and profitable commercialization of next-generation solar cells.

Ideally, final compounds could be obtained by following two strategies (**Figure 7**): a) functionalization of the unsubstituted spirobifluorene core via halogenation, nitration or acylation, and subsequent addition of the desired functional groups through selected reactions; b) construction of the spiro-linkage using pre-functionalized precursors (e.g., substituted 2-halobiphenyls and fluorenones).

Currently, the first strategy is the most used. Indeed, halogen and amino intermediates have been extensively prepared by exploiting the reactivity of 2, 2′, 7, and 7′ positions of 9,9′-spirobifluorene, and nowadays are commercially available thanks to the growing interest on spirobifluorene-based materials in recent years (**Table 2**).[32] It is worth noting that by direct reaction of the spirobifluorene, the 2,2′,7,7′-tetrasubstituted and 2,2′-disubstituted precursors can be achieved with moderate to good yields, while the 2,7-disubstitution is not accessible due to the higher reactivity toward a second functionalization of the 2′ position respect to the 7 position.

Halogen precursors are widely employed as starting materials for metal-catalyzed amination and cross-coupling reactions that offer many possibilities of functionalization. Indeed, the easy and

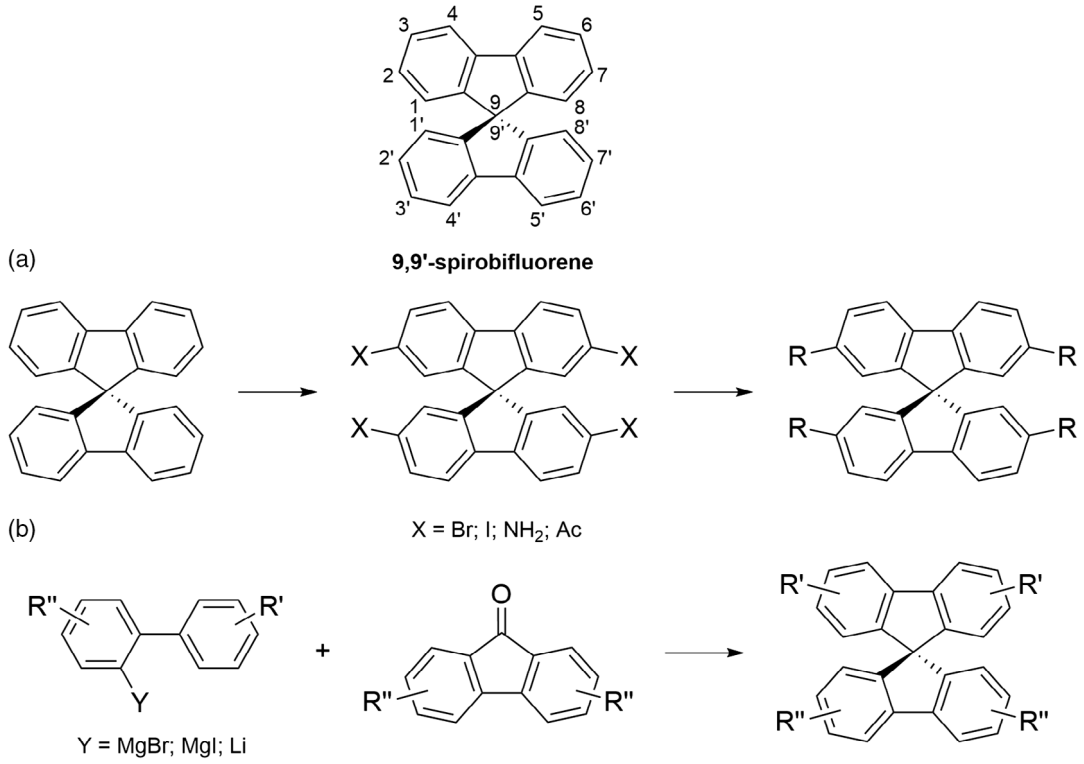

Figure 7. Numbering of 9,9′-spirobifluorene positions and possible synthetic routes to obtain hole-transport materials (HTMs): a) functionalization of the unsubstituted spirobifluorene core and subsequent addition of functional groups, b) construction of the spiro-linkage using prefunctionalized precursors.

© 2023 The Authors. Solar RRL published by Wiley-VCH GmbH

2367198x, 0, Downloaded from https://onlinelibrary.wiley.com/doi/10.1002/solr.202201108 by University Studi Milano Bicocca, Wiley Online Library on [22/02/2023]. See the Terms and Conditions (https://onlinelibrary.wiley.com/terms-and-conditions) on Wiley Online Library for rules of use; OA articles are governed by the applicable Creative Commons License

Table 2. Best reported yields for the preparation of common precursors from 9,9′-spirobifluorene and their current indicative commercial cost.

Precursor	Reagents	Yield [%]	Ref.	Commercial cost [€ g^{-1}][a)]
2,2′,7,7′-tetrabromo-9,9′-spirobifluorene	$Br_2/FeCl_3$	100	[43]	5
2,2′-dibromo-9,9′-spirobifluorene	$Br_2/FeCl_3$	88	[34]	15
2,2′,7,7′-tetraiodo-9,9′-spirobifluorene	I_2/HIO_3	87	[43]	300
2,2′-diiodo-9,9′-spirobifluorene	1) HNO_3/AcOH; 2) $NaBH_4$/Pd/C; 3) a: $NaNO_2$ $HCl_{(aq)}$ b: KI	35	[44]	500
9,9′-spirobifluorene-2,2′,7,7′-tetramine	1) HNO_3; 2) $SnCl_2/HCl_{(aq)}$	90	[45]	150
9,9′-spirobifluorene-2,2′-diamine	1) HNO_3/AcOH; 2) $NaBH_4$/Pd/C;	47	[46]	200

[a)]Indicative for gram scale from popular chemical suppliers.

economic preparation of 2,2′,7,7′-tetrabromo-9,9′-spirobifluorene makes it the most used intermediate.[15,16,18–22,25,27,28] However, looking to a large-scale production, the tetra metal–catalyzed functionalization turns out to be the weakest point due to several drawbacks, such as the need of high substrate/catalyst ratio, generally low yields, and the necessity of chromatographic purification. In contrast, disubstituted derivatives are far less explored, even if their precursor, the 2,2′-dibromo-9,9′-spirobifluorene, is accessible and relative cheap. Moreover, a double functionalization could be more efficient due to the reduced number of byproducts being formed. It is noteworthy that 2,2′-disubstituted spirobifluorenes display a C_2 symmetry, thus they are optically active. Clearly, a resolution process is far from being economic, but the use of an optically pure material instead of the corresponding racemate could affect the molecular packing of HTMs, and hence the final device performances.

Iodo-precursors are not worthy of attention: the reactivity is more or less the same as bromo-precursors, their preparation is less effective, the commercial cost is much higher, and precursor′s molecular weight increases.

Amino precursors proved to be appealing intermediates to avoid metal-catalyzed reactions. For example, the synthesis of **V1305**, **V1306**, **V1307**, and **V1308** was achieved by means of a metal-free condensation reaction carried out without the need of inert atmosphere,[24] but this synthetic approach shows low yields and requires a chromatographic purification too. Nevertheless, this method could be the right strategy to achieve cheap synthetic pathways for the large-scale production of HTMs. It is worth emphasizing that the preparation of the starting intermediates 9,9′-spirobifluorene-2,2′,7,7′-tetramine and 9,9′-spirobifluorene-2,2′-diamine requires a double-step synthesis involving harsh nitration conditions and subsequent reduction of nitro groups, and their cost is more than ten times higher than the corresponding bromo compounds. New effective procedures for the preparation of amino precursors are indeed desirable. In this context, we recently reported a regioselective nitration of 9,9′-spirobifluorene under mild conditions with high yields.[33]

The second strategy, that is, the construction of the spiro-linkage using pre-functionalized precursors, can give access to spiro derivatives with a substitution pattern other than monosubstituted, 2,2′-disubstituted, and 2,2′,7,7′-tetrasubstituted, which are only accessible to the direct functionalization of 9,9′-spirobifluorene. For example, the 2,7-dibromo-9,9′-spirobifluorene can be obtained from 2-bromobiphenyl and 2,7-dibromo-9-fluorenone.[34] By using appropriate precursors, nonconventional substitution patterns could be ideally explored as well as nonsymmetric derivatives.[35] However, the synthetic procedure to obtain the spiro-linkage has not be improved over the years since the first report by Clarkson and Goldberg in 1930,[36] which involves the reaction of *ortho*-metalated 2-halogenobiphenyl with fluorenone to give a fluorenol intermediate, subsequently condensed in boiling acetic acid in presence of a catalytic amount of HCl to give the 9,9′-spirobifluorene. These conditions discourage the use of this strategy, mainly due to functional groups compatibility. Only very recently alternative pathways have been reported in the literature. In 2022, Xu and coworkers reported an unusual reactivity of 1,1-diarylmethylamines in presence of an excess of iodoarenes, using hexafluoroisopropanol as solvent at 140 °C and Pd/Ag catalysis, to form spirobifluorene derivatives in one step reaction via C–H arylation/deaminative annulation.[37] The same year, Beverina et al. claimed a new cheaper and environmental friendly preparation of 9,9′-spirobifluorene by coupling dibenzo[*b*,*d*]thiophene-5,5-dioxide with fluorene.[38] However, the conditions used in these works are far from being mild, and the functional groups compatibility issues are not solved to date.

3. Conclusions and Prospects

The role of the HTMs to achieve high-performance new-generation solar cells is pivotal. In the field of hybrid PSCs, the use of spiro-OMeTAD as HTM allows obtaining outstanding achievements with efficiency exceeding 25%. However, pristine spiro-OMeTAD suffers from low hole mobility and HOMO level that do not fit properly with the level of the perovskite. Moreover, the employment of PSCs with conventional architecture (n–i–p) requires HTMs with high hydrophobicity to protect the perovskite layer from moisture. Furthermore, other features such as high production costs, difficult purification steps, and short-term stability hinder the production and commercialization of large-area spiro-OMeTAD-based PSCs. Although the use of a series of doping materials has been successfully developed to overcome some of these limitations,[6,39] the aggregation of dopants during the film formation affects the stability and the performance of the perovskite-based photovoltaic devices. Under this point of view, an enhancement of the research on dopant-free HTMs for PSCs is desirable. In fact, the absence of dopant species would simplify

© 2023 The Authors. Solar RRL published by Wiley-VCH GmbH

2367198x, 0, Downloaded from https://onlinelibrary.wiley.com/doi/10.1002/solr.202201108 by University Studi Milano Bicocca, Wiley Online Library on [22/02/2023]. See the Terms and Conditions (https://onlinelibrary.wiley.com/terms-and-conditions) on Wiley Online Library for rules of use; OA articles are governed by the applicable Creative Commons License

the production of PSCs and will decrease the presence of undesirable side effects that affect the performance of the devices.

The development of spirobifluorene-based alternative compounds to spiro-OMeTAD benefits of the high thermal stability of this organic material arising from the presence of the sp^3-hybridized spiro-carbon connecting two fluorene units. The recent applied strategy to substitute either partially or totally the eight methoxyphenyl groups of the spiro-OMeTAD with various substituents displayed positive outcomes on the PCE values as well as on the long-term stability of the conventional PSCs, even if the data are strictly connected with the nature of used perovskite. The nature of the substituents plays a pivotal role on the performance of the photovoltaic device. The use of weaker donor substituents with extended π-conjugation than 4-methoxyphenyl induces a decrease on the HOMO level, whereas the introduction of functional groups with strong donating character affects the energy of the HOMO in the opposite direction. To achieve improved efficiency of HTMs, it is important to reduce the gap between the HOMO levels of the HTM and the active layer to facilitate the injection of holes from the perovskite layer. Nonetheless, the tetrasubstituted spirobifluorene remains a challenging substrate to be produced in large scale due to the high number of side products forming during reactions. It is worth to note the impact of the starting reagent on the final production costs. Indeed, the tetrabromo derivatives are cheaper than the tetramine used for the preparation of enamines, but it requires palladium-catalyzed reactions to form the desired products.

A valuable alternative to this approach seems to be the use of disubstituted spirobifluorenes, which have the advantage of reducing the number of side products and their purification. Moreover, the reported studies showed that the efficiency and the stability of the devices are comparable with the benchmark compound, thus they offer novel possible development of HTMs. Although fluorene may offer similar chemical benefits to the 2,7-disubstituted-spirobifluorene, it is worth emphasizing that the presence of two aromatic cycles bound together at the position 9 in the spirobifluorene core greatly reduces the occurrence of unwanted oxidation processes, which usually occur in fluorene-based compounds with formation of 9-fluorenone derivatives.

In addition, organic chemists can explore novel synthetic strategies to improve the preparation of spirobifluorene intermediates in terms of efficiency and environmental impact of the reactions to reduce the costs and the pollution of the production processes of HTMs. These two aspects play a pivotal role on the large-scale diffusion of the photovoltaic devices.

By discussing the environmental impact of the PSCs, it will be advantageous also to report studies testing different HTMs in lead-free perovskite devices to see how the optical and electrical properties of the spirobifluorene derivatives fit with other PSCs. The recent literature does not report new investigations on this subject, indicating the open possibility for many research groups to work in this unexplored field.

Similar to the PSCs, OSCs exhibit the best performance if fabricated under regular architecture. However, this configuration is limited by the high-quality encapsulation technology that prevents a rapid decrease on the stability of the devices. The use of solar cells with inverted configuration appears as a very progressive alternative in term of stability of the devices.[40] Moreover, the PCE and the stability of inverted devices can exhibit values comparable with the conventional architecture, as recently demonstrated.[41] In inverted OSCs, the deposition of HTMs from aqueous solution is desirable because it reduces the problem of the solvent orthogonality referred to the active layer, which is usually deposited from organic solvents. In contrast, inverted PSCs suffer from the hygroscopic (and acid) character of PEDOT:PSS that affects the stability of the resultant devices. This means that aqueous solutions are less prone to be used during the layer deposition. However, in some cases, trace water is helpful to control the crystallization process for obtaining high-quality perovskite films with improved device performance or perovskite quantum dots with high photoluminescence efficiency.[42] Under this point of view, more studies are required to understand if the deposition of HTMs from aqueous solutions, especially in inverted configuration, could be beneficial for the performance of the PSCs. As consequence, the preparation and investigation of water soluble spirobifluorene derivatives in next-generation solar cells appears as very attractive field of research. Furthermore, it is worth to emphasize that the employment of aqueous solutions or, in alternative, ethanol as solvents for the formation of films will have an immense impact of the large production of the solar cells. Within this vision, organic chemists are stimulated to expand the palette of HTMs for PSCs and OSCs soluble in ethanol and water, which will reduce the impact of the solvent in terms of environmental impact.

Acknowledgements

F.R. thanks the Deutsche Forschungsgemeinschaft (DFG) (grant number RI 2635/6-1, project number: 464509280) for funding.

Open Access funding enabled and organized by Projekt DEAL.

Conflict of Interest

The authors declare no conflict of interest.

Keywords

bulk heterojunction solar cells, hole transporting materials, perovskites, solar cells, spirobifluorenes, spiro-OMeTAD

Received: December 15, 2022
Revised: January 3, 2023
Published online:

[1] K. Yoshikawa, H. Kawasaki, W. Yoshida, T. Irie, K. Konishi, K. Nakano, T. Uto, D. Adachi, M. Kanematsu, H. Uzu, K. Yamamoto, *Nat. Energy* **2017**, *2*, 17032.

[2] National Renewable Energy Laboratory, Best Research-Cell Efficiency Chart, https://www.nrel.gov/pv/cell-efficiency.html (accessed: December 2022).

[3] U. Bach, D. Lupo, P. Comte, J. E. Moser, F. Weissörtel, J. Salbeck, H. Spreitzer, M. Grätzel, *Nature* **1998**, *395*, 583.

[4] a) G. Tumen-Ulzii, T. Matsushima, C. Adachi, *Energy Fuels* **2021**, *35*, 18915; b) S.-Y. Jeong, H.-S. Kim, N.-G. Park, *ACS Appl. Mater.*

© 2023 The Authors. Solar RRL published by Wiley-VCH GmbH

2367198x, 0, Downloaded from https://onlinelibrary.wiley.com/doi/10.1002/solr.202201108 by University Studi Milano Bicocca, Wiley Online Library on [22/02/2023]. See the Terms and Conditions (https://onlinelibrary.wiley.com/terms-and-conditions) on Wiley Online Library for rules of use; OA articles are governed by the applicable Creative Commons License

Interfaces **2022**, *14*, 34220; c) Z. Hawash, L. K. Ono, Y. Qi, *Adv. Mater. Interfaces* **2018**, *5*, 1700623.
[5] a) J. J. Yoo, G. Seo, M. R. Chua, T. G. Park, Y. Lu, F. Rotermund, Y. K. Kim, C. S. Moon, N. J. Jeon, J. P. Correa-Baena, V. Bulovic, S. S. Shin, M. G. Bawendi, J. Seo, *Nature* **2021**, *590*, 587; b) H. Min, D. Y. Lee, J. Kim, G. Kim, K. S. Lee, J. Kim, M. J. Paik, Y. K. Kim, K. S. Kim, M. G. Kim, T. J. Shin, S. Il Seok, *Nature* **2021**, *598*, 444; c) J. Jeong, M. Kim, J. Seo, H. Lu, P. Ahlawat, A. Mishra, Y. Yang, M. A. Hope, F. T. Eickemeyer, M. Kim, Y. J. Yoon, I. W. Choi, B. P. Darwich, S. J. Choi, Y. Jo, J. H. Lee, B. Walker, S. M. Zakeeruddin, L. Emsley, U. Rothlisberger, A. Hagfeldt, D. S. Kim, M. Grätzel, J. Y. Kim, *Nature* **2021**, *592*, 381.
[6] G. Ren, W. Han, Y. Deng, W. Wu, Z. Li, J. Guo, H. Bao, C. Liu, W. Guo, *J. Mater. Chem. A* **2021**, *9*, 4589.
[7] P. Murugan, T. Hu, X. Hu, Y. Chen, *J. Mater. Chem. A* **2022**, *10*, 5044.
[8] S. Gangala, R. Misra, *J. Mater. Chem. A* **2018**, *6*, 18750.
[9] T. H. Schloemer, J. A. Christians, J. M. Luther, A. Sellinger, *Chem. Sci.* **2019**, *10*, 1904.
[10] Y. Liu, Y. Hu, X. Zhang, P. Zeng, F. Li, B. Wang, Q. Yang, M. Liu, *Nano Energy* **2020**, *70*, 104483.
[11] a) E. Kasparavicius, A. Magomedov, T. Malinauskas, V. Getautis, *Chem. Eur. J.* **2018**, *24*, 9910; b) N. A. N. Ouedraogo, G. O. Odunmbaku, B. Guo, S. Chen, X. Lin, T. Shumilova, K. Sun, *ACS Appl. Mater. Interfaces* **2022**, *14*, 34303.
[12] G. Li, J. Song, D. Wang, W. Sun, J. Wu, Z. Lan, *J. Power Sources* **2021**, *481*, 229149.
[13] X. Liu, B. Zheng, L. Shi, S. Zhou, J. Xu, Z. Liu, J. S. Yun, E. Choi, M. Zhang, Y. Lv, W.-H. Zhang, J. Huang, C. Li, K. Sun, J. Seidel, M. He, J. Peng, X. Hao, M. Green, *Nat. Photon.* **2022**, *17*, 96.
[14] N. J. Jeon, H. Na, E. H. Jung, T.-Y. Yang, Y. G. Lee, G. Kim, H.-W. Shin, S. Il Seok, J. Lee, J. Seo, *Nat. Energy* **2018**, *3*, 682.
[15] Z. Deng, M. He, Y. Zhang, F. Ullah, K. Ding, J. Liang, Z. Zhang, H. Xu, Y. Qiu, Z. Xie, T. Shan, Z. Chen, H. Zhong, C.-C. Chen, *Chem. Mater.* **2021**, *33*, 285.
[16] Y. Liang, J. Chen, X. Zhang, M. Han, R. Ghadari, N. Wu, Y. Wang, Y. Zhou, X. Liu, S. Dai, *J. Mater. Chem. C* **2022**, *10*, 10988.
[17] D. Poplavskyy, J. Nelson, *J. Appl. Phys.* **2003**, *93*, 341.
[18] M. Jeong, I. W. Choi, K. Yim, S. Jeong, M. Kim, S. J. Choi, Y. Cho, J.-H. An, H.-B. Kim, Y. Jo, S.-H. Kang, J.-H. Bae, C.-W. Lee, D. S. Kim, C. Yang, *Nat. Photon.* **2022**, *16*, 119.
[19] M. Jeong, I. W. Choi, E. M. Go, Y. Cho, M. Kim, B. Lee, S. Jeong, Y. Jo, H. W. Choi, J. Lee, J.-H. Bae, S. K. Kwak, D. S. Kim, C. Yang, *Science* **2020**, *369*, 1615.
[20] Z. Zhang, L. Yuan, B. Li, H. Luo, S. Wang, Z. Li, Y. Xing, J. Wang, P. Dong, K. Guo, Z. Wang, K. Yan, *Sol. RRL* **2022**, *6*, 2100944.
[21] B. Zhao, T. Zhang, C. Liu, Z. Li, W. Liu, Y. Bai, T. Wang, X. Sun, S. Zhu, Y. Chen, Z. Liu, H. Liu, T. Liu, X. Li, *Mater. Today Energy* **2022**, 101191.
[22] X. Zhang, X. Liu, N. Wu, R. Ghadari, M. Han, Y. Wang, Y. Ding, M. Cai, Z. Qu, S. Dai, *J. Energy Chem.* **2022**, *67*, 19.
[23] Z. Hu, W. Fu, L. Yan, J. Miao, H. Yu, Y. He, O. Goto, H. Meng, H. Chen, W. Huang, *Chem. Sci.* **2016**, *7*, 5007.
[24] D. Vaitukaityte, C. Momblona, K. Rakstys, A. A. Sutanto, B. Ding, C. Igci, V. Jankauskas, A. Gruodis, T. Malinauskas, A. M. Asiri, P. J. Dyson, V. Getautis, M. K. Nazeeruddin, *Chem. Mater.* **2021**, *33*, 6059.
[25] A. Jegorovė, C. Momblona, M. Daškevičienė, A. Magomedov, R. Degutyte, A. M. Asiri, V. Jankauskas, A. A. Sutanto, H. Kanda, K. Brooks, N. Klipfel, M. K. Nazeeruddin, V. Getautis, *Sol. RRL* **2022**, *6*, 2100990.
[26] M. Han, Y. Liang, J. Chen, X. Zhang, R. Ghadari, X. Liu, N. Wu, Y. Wang, Y. Zhou, Y. Ding, M. Cai, H. Chen, S. Dai, *ChemSusChem* **2022**, *15*, e202201485.
[27] N. Onozawa-Komatsuzaki, D. Tsuchiya, S. Inoue, A. Kogo, T. Funaki, M. Chikamatsu, T. Ueno, T. N. Murakami, *ACS Appl. Energy Mater.* **2022**, *5*, 6633.
[28] Y. Liu, F. Liu, J. Wang, H. Huang, S. Yan, S. Gao, L. Wang, W. Huang, T. Qin, *Dyes Pigm.* **2021**, *188*, 109164.
[29] Y. Wang, W. Chen, L. Wang, B. Tu, T. Chen, B. Liu, K. Yang, C. W. Koh, X. Zhang, H. Sun, G. Chen, X. Feng, H. Y. Woo, A. B. Djurišić, Z. He, X. Guo, *Adv. Mater.* **2019**, *31*, 1902781.
[30] S. Ameen, M. S. Akhtar, M. Nazim, E.-B. Kim, M. K. Nazeeruddin, H.-S. Shin, *Electrochim. Acta* **2019**, *319*, 885.
[31] T. Matsumoto, T. Murakami, F. Schlüter, H. Murata, V. Vohra, F. Rizzo, *Sol. RRL* **2022**, *6*, 2100661.
[32] a) L. Vaghi, F. Rizzo, J. Pedrini, A. Mauri, F. Meinardi, U. Cosentino, C. Greco, A. Monguzzi, A. Papagni, *Photochem. Photobiol. Sci.* **2022**, *21*, 913; b) F. Schlüter, B. J. Ravoo, F. Rizzo, *J. Mater. Chem. B* **2019**, *7*, 4933; c) G. Bottaro, F. Rizzo, M. Cavazzini, L. Armelao, S. Quici, *Chem. Eur. J.* **2014**, *20*, 4598; d) H. C. Schmidt, C. B. Larsen, O. S. Wenger, *Angew. Chem. Int. Ed.* **2018**, *57*, 6696; e) Y. Zhou, Y. Li, R. Zhang, D. Zhao, Q. Yan, *Chem. Asian J.* **2021**, *16*, 1893.
[33] Unpublished results.
[34] J. Pei, J. Ni, X.-H. Zhou, X.-Y. Cao, Y.-H. Lai, *J. Org. Chem.* **2002**, *67*, 4924.
[35] C. Poriel, L. Sicard, J. Rault-Berthelot, *Chem. Commun.* **2019**, *55*, 14238.
[36] R. G. Clarkson, M. Gomberg, *J. Am. Chem. Soc.* **1930**, *52*, 2881.
[37] Y. Wu, F.-W. Wu, K. Zhou, Y. Li, L. Chen, S. Wang, Z.-Y. Xu, S.-J. Lou, D.-Q. Xu, *Chem. Commun.* **2022**, *58*, 6280.
[38] S. Mattiello, G. Lucarelli, A. Calascibetta, L. Polastri, E. Ghiglietti, S. K. Podapangi, T. M. Brown, M. Sassi, L. Beverina, *ACS Sustain. Chem. Eng.* **2022**, *10*, 4750.
[39] Y. Shen, K. Deng, L. Li, *Small Methods* **2022**, *6*, 2200757.
[40] Y. Yao, C. Cheng, C. Zhang, H. Hu, K. Wang, S. De Wolf, *Adv. Mater.* **2022**, *34*, 2203794.
[41] a) Q. Jiang, J. Tong, Y. Xian, R. A. Kerner, S. P. Dunfield, C. Xiao, R. A. Scheidt, D. Kuciauskas, X. Wang, M. P. Hautzinger, R. Tirawat, M. C. Beard, D. P. Fenning, J. J. Berry, B. W. Larson, Y. Yan, K. Zhu, *Nature* **2022**, *611*, 278; b) J. H. Heo, S. Lee, H. J. Lee, J. K. Park, Y. Lee, S. Y. Hong, W.-S. Han, S. H. Im, *Sol. RRL* **2022**, *6*, 2200573.
[42] a) G. E. Eperon, S. N. Habisreutinger, T. Leijtens, B. J. Bruijnaers, J. J. van Franeker, D. W. deQuilettes, S. Pathak, R. J. Sutton, G. Grancini, D. S. Ginger, R. A. J. Janssen, A. Petrozza, H. J. Snaith, *ACS Nano* **2015**, *9*, 9380; b) S. Cheng, H. Zhong, *J. Phys. Chem. Lett.* **2022**, *13*, 2281.
[43] R. Wu, J. S. Schumm, D. L. Pearson, J. M. Tour, *J. Org. Chem.* **1996**, *61*, 6906.
[44] F. Thiemann, T. Piehler, D. Haase, W. Saak, A. Lützen, *Eur. J. Org. Chem.* **2005**, *2005*, 1991.
[45] I. Pyka, D. Ryvlin, S. R. Waldvogel, *ChemPlusChem* **2016**, *81*, 926.
[46] Y. Sun, X. Zhao, G. Zhu, M. Li, X. Zhang, H. Yang, B. Lin, *Electrochim. Acta* **2020**, *333*, 135495.

© 2023 The Authors. Solar RRL published by Wiley-VCH GmbH

2367198x, 0, Downloaded from https://onlinelibrary.wiley.com/doi/10.1002/solr.202201108 by University Studi Milano Bicocca, Wiley Online Library on [22/02/2023]. See the Terms and Conditions (https://onlinelibrary.wiley.com/terms-and-conditions) on Wiley Online Library for rules of use; OA articles are governed by the applicable Creative Commons License